Int. J. Multiphase Flow Vol. 14, No. 6, pp. 655–677, 1988
Printed in Great Britain.

0301-9322/88 $3.00 + 0.00

THE WAVE DYNAMICS OF A VAPOUR–LIQUID MEDIUM

V. E. NAKORYAKOV, B. G. POKUSAEV, I. R. SHREIBER and N. A. PRIBATURIN
Institute of Thermophysics of the Siberian Branch of the U.S.S.R. Academy of Sciences, 630090 Novosibirsk, U.S.S.R.

(*Received* 5 *February* 1987; *in revised form* 10 *July* 1988)

Abstract—New wave models for a bubble vapour–liquid medium and methods to specify interphase heat transfer are suggested. The evolution of vapour bubbles in a pressure wave and the connection of the wave structure and dynamics with this evolution have been studied. A wide range of experiments have been conducted to investigate the structure and dynamics of pressure waves. New results for solving the basic model equations for waves in a vapour–liquid medium are also presented and these solutions are compared with the experimental data obtained.

Key Words: vapour liquid media, vapour bubbles heat flux, pressure wave, sound speed, attenuation dispersive relation, phase velocity, bubble collapse, shock wave, model equation

1. INTRODUCTION

Vapour–liquid flows are the most widely spread working medium in up-to-date energetic apparatus. The pioneering investigations of the fundamental characteristics of such a two-phase medium (sound velocity, in particular), started by Viglin (1938), Avdonin & Novikov (1960), Sychev (1961), Semyonov & Kosterin (1964), Grolmes & Fauske (1968), Ardron & Duffey (1979), Mecredy & Hamilton (1972), Radovskii (1979), Deich *et al.* (1964), Kutateladze *et al.* (1979) and Nigmatulin (1982), have shown that in such a medium the sound velocity is low and that the thermal relaxation and strong nonlinearity due to the high compressibility of the medium play an important role.

Thus calculations of the evolution of a vapour–liquid medium require, even for high velocities, mainly gas dynamic methods. The traditional gas dynamic methods do not allow one to take into account the most important specific characteristics of a two-phase medium (phase transitions, inertia of vapour inclusions). So the investigations presented here may be considered as an attempt to create the fundamentals of the nontraditional gas dynamics of a vapour–liquid medium, which allows one, if only as a first approximation, to take into account the basic peculiarities of the vapour–liquid medium, heat transfer processes on the boundary, dissipation and inertial properties of vapour inclusions.

2. EQUILIBRIUM MODEL

Let us describe the theory of wave propagation in a liquid with vapour bubbles, beginning with the analysis of the equilibrium wave model. Preliminarily we will introduce general equations and basic relations for the homogeneous bubble–suspension model. Further, we will use the homogeneous vapour–liquid bubble–suspension model, since it seems suitable to study the wave processes in such media (Wijngaarden 1968; Kuznetsov *et al.* 1978).

The homogeneous bubble–suspension model assumes that the mixture density $\rho = \rho_L(1-\epsilon) + \rho_G\epsilon$ or $1/\rho = [(1-X)/\rho_L] + V$, where ρ_L = liquid density, ρ_G = vapour density, $\epsilon = V\cdot\rho$, where V = specific volume of the vapour in the mixture, ϵ = void fraction and X = quality.

X is defined as $X = V\cdot\rho_G$ or $X = \rho_G\epsilon/[\rho_G\epsilon + \rho_L(1-\epsilon)]$. It is also useful to present a relation for the variation of the gas volume ΔV and that of the density $\Delta\rho$:

$$\frac{\Delta V}{V} = \frac{\Delta p(1-\epsilon)^2(1-X)}{c_L^2\rho\epsilon} - \frac{\Delta\rho}{\rho\epsilon},$$

where c_L is the second velocity of the liquid. Here we have used the acoustic relation between a liquid density perturbation ($\Delta\rho$) and a pressure perturbation (Δp) in the medium: $\Delta\rho_L = \Delta p/c_L^2$.

Let us define the thermodynamic characteristics of this mixture: the entropy $s = s_L(1 - X) + s_G X$, where s_L and s_G are the entropies of the liquid and of the vapour phase; and the enthalpy $i = i_L(1 - X) + i_G X$. The equations for the evolution of the bubble mixture are as follows:

$$\frac{\partial r}{\partial t} + \frac{\partial}{\partial x}(\rho u) = 0,$$

$$\frac{\partial u}{\partial t} + u\frac{\partial u}{\partial x} = -\left(\frac{1}{\rho}\right)\frac{\partial p}{\partial x}, \qquad [1]$$

$$\frac{\partial i}{\partial t} + u\frac{\partial i}{\partial x} = \left(\frac{1}{\rho}\right)\left(\frac{\partial p}{\partial t} + u\frac{\partial p}{\partial x}\right).$$

Here u = perturbation of velocity and $p = p_0 + \Delta\rho$ = pressure of the mixture. The experience of studying waves in a liquid with gas bubbles has shown that due to the high compressibility of the mixture, the nonlinearity in the original hydrodynamic equations may be omitted. The dependence of the sound velocity c on the amplitude of perturbations is considered to be the main source of the nonlinearity of the problem, i.e. the main contribution to the nonlinearity is due to the equation of state (Nakoryakov *et al.* 1975). We will also adhere to this concept in analysing waves propagating in a liquid with vapour bubbles.

The linearized system [1] can be reduced to the equation

$$\frac{\partial^2 \rho}{\partial t^2} = \frac{\partial^2 p}{\partial x^2}, \qquad [2]$$

and to the adiabatic condition in the mixture during wave propagation, $ds/dt = 0$. The relation between p and density ρ in [2] is the crucial moment in the wave dynamics of two-phase media. In particular, studying the wave propagation in a liquid with gas bubbles, it was pointed out that this relation is of a relaxational nature (Kogarko 1961; Nakoryakov *et al.* 1972) $p = p(\rho, \dot{\rho}, \ddot{\rho})$, whose concrete form can be determined from the dynamic and solitary-inclusion energy equations. For a gas–liquid medium this relation can be obtained in terms of the approximation of the adiabatic character of bubble fluctuations, from the Rayleigh equation for a solitary bubble:

$$R\ddot{R} + \frac{3}{2}(\dot{R})^2 = \frac{p(R) - p_\infty}{\rho_L}, \qquad [3]$$

where

$$p(R) = p_0\left(\frac{R_0}{R}\right)^{3\gamma} + \frac{4\nu}{3}\frac{\dot{R}}{R},$$

p_∞ = pressure in the mixture,

ν_L = liquid viscosity

and

R_0 = initial radius of a bubble.

Considering the elementary relations of the homogeneous model, [3] can be reduced to

$$\Delta p = c^2 \Delta\rho + 2\eta\dot{\rho} + 2\beta\ddot{\rho}, \qquad [4]$$

where

$$c^2 = c_0^2 + c_0^2\frac{\delta + 1}{\rho_0 \epsilon_0}\Delta\rho, \qquad [5]$$

$$c_0 = \left[\frac{\delta p_0}{\rho\epsilon_0(1 - \epsilon_0)}\right]^{1/2} = \text{sound velocity in the mixture},$$

$$\eta = \frac{2\nu_L}{3\epsilon_0},$$

$$\beta = \frac{R_0^2}{6\epsilon_0(1-\epsilon_0)},$$

ϵ_0 = initial void fraction

and

γ = ratio of specific heats.

In the equilibrium model considered we will limit ourselves to the long-wave approximation and neglect the relaxation effects. Then, it follows from [2] that

$$\frac{\partial^2 p}{\partial t^2} - \left(\frac{\partial p}{\partial \rho}\right)_s \frac{\partial^2 p}{\partial x^2} = 0. \qquad [6]$$

Let us consider what represents $(\partial p/\partial \rho)_s$ in a vapour–liquid medium. The solution of such a problem can be found in the book by Landau & Lifshits (1953). Let us determine, using thermodynamic analysis, the expression for the derivative $(\partial p/\partial \rho) = c^2$. The basic assumption of the equilibrium model is the instantaneous establishment of the vapour–liquid equilibrium with a perturbation superimposed, $T_L = T_G$. Physically, the density variation process in the mixture with a pressure perturbation superimposed is as follows. A pressure variation Δp causes an overheat ΔT in the system, which is found from the Clapeyron–Clausius equation:

$$\frac{dp_G}{dT_G} = \frac{L}{T\left(\frac{1}{\rho_G} - \frac{1}{\rho_L}\right)}, \qquad [7]$$

where L = latent heat of evaporation. The overheat ΔT brings about either evaporation or condensation on the boundary. Naturally, it leads to a change in the bubble radius ΔR. It means that the vapour volume ΔV and the mixture density $\Delta \rho$ change. So the factor of $\Delta \rho$, varying due to Δp is $(\partial p/\partial \rho)_s$. Thus, in varying Δp, only X varies in the system, and ρ_L and ρ_G do not vary and are not functions of Δp. Using the definition of ρ in terms of X, we can write

$$\left(\frac{\partial \rho}{\partial p}\right)_s = -\rho^2\left(\frac{1}{\rho_G} - \frac{1}{\rho_L}\right)\left(\frac{\partial X}{\partial p}\right)_s. \qquad [8]$$

To calculate the derivative $(\partial X/\partial p)_s$ we will use some thermodynamic relations. The entropy of the mixture in the wet-vapour region is determined by two independent parameters near the saturation line—X and the temperature T. In this model the temperatures of the phase are equal. Then,

$$ds = \left(\frac{ds}{dT}\right)_X dT + \left(\frac{ds}{dX}\right)_T dX. \qquad [9]$$

It follows from the definition of the entropy that

$$\left(\frac{\partial s}{\partial T}\right)_X = X\left(\frac{\partial s_G}{\partial T}\right)_X + (1-X)\left(\frac{\partial s_L}{\partial T}\right)_X. \qquad [10]$$

For the liquid on the saturation line $ds_L/dT = C_L/T$ and for the vapour $ds_G/dT = C_G T$, where C_L and C_G are the heat capacities of the liquid and the vapour, respectively.

Then

$$\left(\frac{ds}{dT}\right)_X = \frac{[XC_G + (1-X)C_L]}{T} = \frac{C_*}{T}, \qquad [11]$$

where $C_* = [XC_G + (1-X)C_L]$. The physical meaning of C_* is the amount of heat needed to increase the temperature of 1 kg of the mixture by 1°C if the dryness factor is the same.

Let us consider the expression

$$\left(\frac{ds}{dX}\right)_T = s_G - s_L = \frac{L}{T}. \qquad [12]$$

For an adiabatic process, when $ds = 0$, we get from [9] considering [10] and [12], that

$$\frac{C_*}{T}\,dT + \frac{L}{T}\,dX = 0. \qquad [13]$$

Using [7], let us replace dT by dp in relation [13],

$$\left(\frac{C_*}{L}\right)\left(\frac{1}{\rho_G} - \frac{1}{\rho_L}\right)dp + \left(\frac{L}{T}\right)dX = 0,$$

and find $(\partial X/\partial p)$:

$$\left(\frac{\partial X}{\partial p}\right) = -\left(\frac{C_* T}{L^2}\right)\left(\frac{1}{\rho_G} - \frac{1}{\rho_L}\right). \qquad [14]$$

The difference between the heat capacities of the dry vapour and of the water on the saturation line $C_G - C_L = (dL/dT) - (L/T)$. Then $C_* = C_L + X[(dL/dT) - (L/T)]$. Far from the critical range $C_L \approx C_{p_L}$ and

$$C_* = C_{p_L} + X\left(\frac{dL}{dT} - \frac{L}{T}\right) \approx C_{p_L} - X\frac{L}{T}. \qquad [15]$$

Substituting [14] into [8] we find

$$\left(\frac{\partial \rho}{\partial p}\right)_s = \frac{\rho^2 C_* T}{\rho_G^2 L^2}. \qquad [16]$$

Using the assumption that the vapour is an ideal gas, i.e. $p_G \rho_G = \mathbf{B} \cdot T$, where $\mathbf{B}$ is the absolute gas constant, we obtain an expression for the square of the sound velocity:

$$\left(\frac{\partial p}{\partial \rho}\right)_s = c_e^2 = \frac{p_G^2 L^2}{\rho^2 C_* \mathbf{B}^2 T^3}. \qquad [17]$$

Substituting approximately $\rho = \rho_L(1 - \epsilon) \approx \rho_L$, $C_* = C_{p_L}$ and $p_2 = p_0$, we obtain

$$c_e^2 = \frac{p_0 L}{\rho_L \sqrt{c_{p_L} T T \mathbf{B}}}. \qquad [18]$$

Expression [18] is sometimes referred to as the thermodynamically equilibrium sound velocity of a vapour–liquid medium. The wave expression [6] assumes the form

$$\frac{\partial^2 p}{\partial t^2} - c_e^2 \frac{\partial^2 p}{\partial x^2} = 0. \qquad [19]$$

If we substitute into [17] the values for the parameters of the steam–water medium which is on the saturation line under normal conditions ($p_0 \sim 10^5$ Pa, $T = 373$ K) for a void fraction of the order of 1%, then the value of the thermodynamically equilibrium sound velocity will be of the order of 1 m/s.

Experiments carried out specially to determine the sound velocity in a bubble vapour–liquid medium have not yielded such low values (Semyonov & Kosterin 1964; Grolmes & Fauske 1968). Nor have our experimental data on the wave propagation in such a two-phase medium enabled us to discover any wave propagation at a velocity defined by [18] (figure 1).

Since in the following we will have to apply to our experiments over and over again, we will describe in this section the respective techniques and methods of measurement. The objective of our experiments was to check the correspondence of the theoretical models developed to the real picture of wave propagation. The respective program of experiments was developed on the basis of this objective.

The experiments were conducted on a special "shock-tube" setup (figure 2). The working section (low-pressure chamber) is separated from a high-pressure chamber by a diaphragm-change unit. The working section comprises interchangeable units, namely a stainless steel pipe with i.d. 52 mm and a wall thickness of 8 mm. To maintain the working temperature of the medium, the working section was placed in thermostat which had a high heat capacity and was heated by electric heaters.

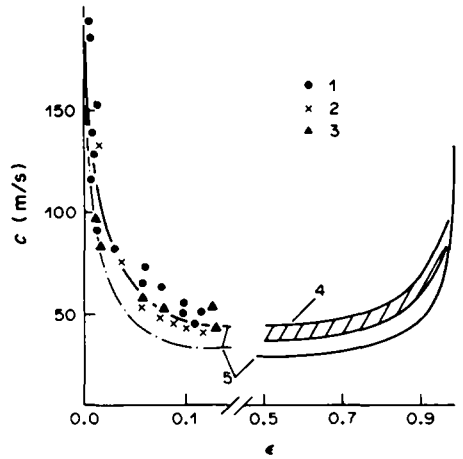

Figure 1. Sound velocity in a liquid with vapour bubbles vs void fraction. Weak compression wave $\Delta p_0/p_0 \simeq 0.1$–$0.2$. 1, Water—$p_0 = 10^5$ Pa; 2, Freon-113, $\Delta p_0/p_0 = 10^5$ Pa; 3, Grolmes & Fauske (1968); 4, Semyonov & Kosterin (1964); 5, calculation.

The temperature of the pipe wall was maintained equal to the temperature of the working medium at a given pressure with an accuracy of 0.5°C.

Vapour bubbles were generated by injecting vapour into the liquid through 0.3 mm dia needle-like capillaries in the lower part of the working section or, otherwise, were created on artificial evaporation centres during boiling. For the latter method, a heating unit was installed

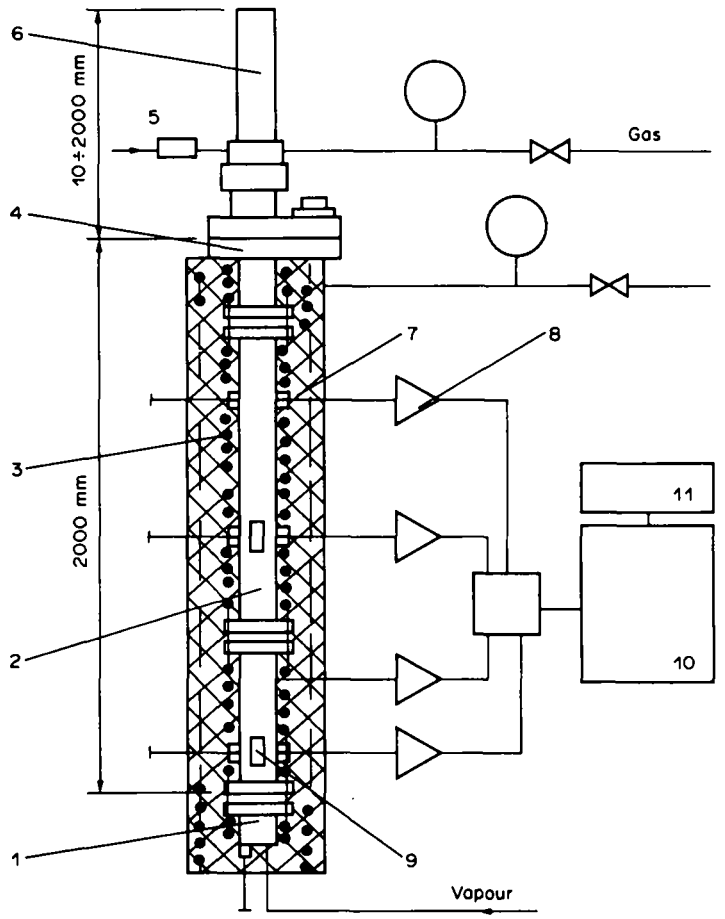

Figure 2. Scheme of the experimental setup. 1, Vapour bubbles generator; 2, test section; 3, thermostat; 4, membrane replacement unit; 5, valve; 6, high-pressure chamber; 7, pressure sensors; 8, amplifiers; 9, optical windows; 10, computer; 11, tape recorder.

below the working section; the power of the heater could vary smoothly. The temperature of the vapour in both cases was controlled by a thermocouple located immediately under the capillaries. The bubble diameter was determined by photography in the middle part of the working section. The most probable value of radius R_0 and the mean square deviation of the bubble dimensions Δ were calculated by statistical techniques. For instance, for the water–steam mixture at static pressure $p_0 = 0.5$ MPa, $R_0 = 1.38$ mm and $\Delta = 0.25$ mm. For the vapour–Freon mixture (Freon-12) at $p_0 = 0.7$ MPa, $R_0 = 1.3$ mm and $\Delta = 0.27$ mm; and at $p_0 = 1.3$ MPa, $R_0 = 0.95$ mm and $\Delta = 0.15$ mm. Experimental data processing and comparison with calculations were made by means of R_0.

The mean void fraction ϵ_0 was determined by changing the upper level of the working section and introducing vapour bubbles therein.

The high-pressure chamber is a 52 mm i.d. stainless steel pipe. The chamber length was varied in our experiments from 5 up to 2000 mm, which allowed us to obtain signals with a different duration of the compression or rarefaction process. The fast diaphragm-change unit allows us, without depressurization of the internal volume of the working section, to change diaphragms which were made of aluminium foil of thicknesses from 0.01 up to 0.3 mm. The use of such diaphragms permitted us to obtain initial pressure drops between the chambers within 0.01–2 MPa. The rupture of a diaphragm could be realized in two ways: spontaneously, when a certain pressure drop had been attained; or by means of a pneumatic knife set.

To change the pressure profile in a perturbation wave, piezoelectric probes whose operating frequencies ranged from 3 Hz to 20 kHz were located along the length of the working section. The signal of the probe was fed to cathode followers whose input resistance was 100 mΩ and had capacity up to 10 pF. Calibration of the pressure probes was carried out on the shock tube filled with air, the temperature and the pressure being equal to the working parameters of the vapour–liquid medium. A detailed description of the measurement technique can be found in Pokusaev *et al.* (1981).

3. TWO-TEMPERATURE MODEL

Analysis of the experiments conducted has shown that the propagation velocity of long-wave perturbations can be well-generalized by the dependence of the sound velocity in a liquid with gas bubbles (Batchelor 1968):

$$c_0 = \left(\frac{\gamma p_0}{\rho_0 \epsilon_0}\right)^{1/2}, \quad \epsilon_0 \ll 1.$$

As for the structure of pressure waves formed in a bubble vapour–liquid medium, it has been found out that both perturbations similar to waves in a gas–liquid medium (Kuznetsov *et al.* 1978) and spreading pressure-wave profiles could appear in this case.

On the basis of these experimental facts, the further theoretical analysis was built up using the two-temperature model. Let us formulate its main assumptions. The bubble–liquid interface is in thermodynamic equilibrium when a wave is propagating, and the Clapeyron–Clausius conditions [7] are valid on the interface. Thus the liquid is a thermostat and preserves, at a sufficient distance from the surface of a bubble, an initial temperature, T_0. The vapour inside the bubble behaves adiabatically. The mixture in question satisfies all the equations and relationships of a homogeneous bubble mixture, which are given in the previous section. The nonlinearity occurring during the propagation of a wave is largely due to the compressibility of the medium.

Let us derive an evolution equation to describe the behaviour of pressure perturbations in a liquid with vapour bubbles. The hydrodynamic equations of the mixture will be taken in a linear form [2]. The equation of the mixture state will be written without allowance for bubble radius variation due to phase transition. This equation is obtained from the dynamic equation of a solitary cavity [3], taking due account of adiabatic vapour behaviour and small amplitudes of bubble volume variation, and is of the form

$$\Delta p = \Delta p_G + \frac{R_0^2}{3\epsilon_0(1-\epsilon_0)} \frac{\partial^2 \rho}{\partial t^2} + 2\eta \frac{\partial \rho}{\partial t}. \qquad [20]$$

Putting aside this equation, the pressure difference between the mixture and the liquid is represented as the deviations from the initial state

$$p_\infty - p(R) = \Delta p - \Delta p_G. \qquad [21]$$

The energy equation for a solitary vapour bubble, with allowance for the mass variability due to phase transition, and the equation of the vapour state are written as follows (Finch & Neppiras 1973):

$$\frac{\partial p_G}{\partial t} + \frac{3\gamma p_G}{R}\frac{\partial R}{\partial t} = \frac{3(\gamma-1)}{R}\left[-q_R - \frac{(L - C_{pG}T)}{4\pi R^2}\frac{dM}{dt}\right], \qquad [22]$$

where q_R is the heat flux on the boundary and π is the vapour mass in a bubble. The vapour mass variation is considered to be completely defined by the amount of heat from the liquid:

$$\frac{dM}{dt} = \frac{4\pi R^2}{L}(q_G = q_L). \qquad [23]$$

Here q_L is the specific heat flux to interphase from the liquid and q_G is the heat flux to the vapour. Supposing that $q_L \gg q_G$, with allowance for [23] we shall obtain

$$\frac{\partial p_G}{\partial t} + \frac{3\gamma P_G}{R}\frac{\partial R}{\partial t} = -\frac{3\gamma P_{G0}}{R\rho_G L}q_L. \qquad [24]$$

This equation written in terms of the mixture density $\rho = \epsilon/(4/3\pi R^3 N)$ (N = the bubble number per unit volume) is of the form

$$\frac{\partial p_G}{\partial t} - \frac{\gamma P_G}{\rho\epsilon}\frac{\partial \rho}{\partial t} = -\frac{3\gamma p_{G0}}{R\rho_G L}q_L. \qquad [25]$$

When deriving [25] it was assumed that $\rho_G \ll \rho_L$, $\rho \approx \rho_L$, $\epsilon \ll 1$, $c_0 < c_L$ and the homogeneous model relations were used,

$$\frac{dV}{dt} = -\frac{1}{\rho^2}\frac{d\rho}{dt}, \quad \frac{dR}{dt} = \frac{1}{4\pi N R^2}\frac{dV}{dt}. \qquad [26]$$

The value $\gamma p/\rho\epsilon$ in [25] is the square of the low-frequency sound velocity (c^2) in a bubble mixture which is defined on the basis of local values for pressure and void fraction in a wave. If this value is expanded into a series of terms of the initial medium state,

$$c^2 = c_0^2 + \left(\frac{\partial c^2}{\partial \rho}\right)_{\rho=\rho_0}\Delta\rho, \qquad [27]$$

then, as has been shown by Nakoryakov *et al.* (1975), [5] is obtained.

Differentiating [25] once with respect to t and using [5], [20] and [2] we reduce the initial system of equations to one equation:

$$\frac{\partial^2 p}{\partial t^2} - c_0^2\frac{\partial^2 p}{\partial x^2} - \frac{\gamma+1}{2\gamma}c_0^2\frac{\partial^2}{\partial x^2}\left(\frac{\Delta p^2}{p_0}\right) = 2\beta\frac{\partial^4 p}{\partial t^2\partial x^2} + 2\eta\frac{\partial^3 p}{\partial t\partial x^2} - \frac{3\gamma p_0}{R\rho_G L}\frac{\partial q_L}{\partial t}. \qquad [28]$$

In the case where there are no phase transitions on the bubble–liquid boundary ($q_L = 0$) (i.e. a liquid with gas bubbles), [28] turns into the Boussinesq equation for a pressure perturbation. In terms of this approximation, the wave dynamics of gas–liquid systems were studied by Gasenko *et al.* (1977).

Equation [28], as the characteristic velocity of wave propagation, contains the value $c_0 = (\gamma\rho_0/\rho_0\epsilon_0)^{1/2}$, so the two-temperature model immediately yields the correct value for the characteristic sound velocity in the vapour–liquid mixture observed in our experiments.

4. HEAT FLUX ON THE BUBBLE–LIQUID BOUNDARY

In the case where phase transitions exist (i.e. $q_L \neq 0$), then the question arises as to how q_L is related to the amplitude of a perturbation p. Practically, the problem consists of determining the

heat flux q_L. To do this, we consider the problem of a temperature field near a bubble of constant radius R_0, the temperature of whose boundary is always on the saturation line and corresponds to the instantaneous pressure value in the system. Approximating the constancy of the boundary of R_0 is suitable for low-intensity perturbations, when the radius of the vapour bubble does not change considerably from its initial value. In the case when $\sqrt{2a_L/\omega} < l$, where a_L = thermal diffusivity of the liquid, ω = frequency of perturbation and l = distance between bubbles, we can assume that at infinity the temperature of the liquid is equal to T_0 (the initial temperature of the liquid). The solution of such a problem is well-known and for the initial conditions $T(0, r) = T_0$, can be written as

$$q_L = \frac{\lambda_L}{\sqrt{\pi a_L}} \int_0^t \frac{\partial T}{\partial t} \frac{d\tau}{\sqrt{t-\tau}}. \quad [29]$$

The temperature perturbation in the boundary, ΔT, is related to the pressure perturbation in the system Δp, by the Clapeyron–Clausius equation [7]. For small pressure perturbations $\Delta p_0/p_0 < 1$, we can assume that $\rho_L = \text{const}$ and

$$\Delta T = \left(\frac{T_0}{\rho_G L}\right) \Delta p. \quad [30]$$

The heat flux $q_L(t)$ can be written in terms of the pressure perturbation in the mixture:

$$q_L = \frac{\rho_L C_{p_L} T_0}{\rho_G L} \sqrt{\frac{a_L}{\pi}} \int_0^t \frac{\partial p}{\partial t} \frac{\partial \tau}{\sqrt{t-\tau}}. \quad [31]$$

It should be noted that such an approach to the determination of q_L does not allow the possibility of obtaining an equilibrium situation. Small as a perturbation may be, $T(t) = T_0$ is always constant, i.e. the model does not possess any mechanism allowing phase temperatures to be equalized. It is obvious that this is due to the fact that the lengths of the heat waves are much smaller than the distances between bubbles and, hence, are much smaller than the length of an acoustic wave. The use of the homogeneous model assumes that the length of an acoustic wave is much greater than the distances between bubbles. In the case where the lengths of the heat waves are of the order of the acoustic ones, then the wave propagation can be considered in terms of the equilibrium model described in the first paragraph. The heat flux q_L can be determined differently, in order to eliminate the restriction imposed on the length of the heat waves.

To determine the heat flux, we will use the cellular model of a vapour–liquid medium (Nigmatulin 1978). We will assume that each bubble of radius R is surrounded by a liquid cell of radius $\mathscr{R}$. For the boundary of this cell we will formulate the adiabatic conditon

$$\left(\frac{\partial T}{\partial r}\right)_{r=\mathscr{R}} = 0, \quad [32]$$

as distinguished from the previous condition $T_{r\to\infty} = T_0$.

The radius of the cell, $\mathscr{R}$, is determined, according to the cellular model, using the void fraction ϵ as follows:

$$\mathscr{R} = R \cdot \epsilon^{-1/3}. \quad [33]$$

The heat flux is found by solving the heat conduction equation for the interval $R \leqslant r \leqslant \mathscr{R}$:

$$\frac{\partial T}{\partial t} = a_L \left(\frac{\partial^2 T}{\partial r^2} + \frac{2}{r}\frac{\partial T}{\partial r}\right). \quad [34]$$

The homogeneous initial condition is $T(r, 0) = T_0$; the boundary conditions are $T(R, t) = T_s(t)$ and [32]. Solving the equation by the Laplace method, we will obtain, considering [30], an image $\mathscr{I}$ for the heat flux on the interphase boundary:

$$\mathscr{I}\left(\lambda_L \frac{\partial T}{\partial r}\right) = G(s_1)\mathscr{I}(\Delta p), \quad [35]$$

where

$$G(s_1)=\frac{\lambda_L T_0}{\rho_G L}\left[\frac{\sqrt{\frac{s_1}{a_L}}\left(\frac{1}{\mathscr{R}}+\sqrt{\frac{s_1}{a_L}}\right)\exp\left(-l\sqrt{\frac{s_1}{a_L}}\right)}{\sqrt{\frac{s_1}{a_L}}\cosh\left(l\sqrt{\frac{s_1}{a_L}}\right)-\frac{1}{\mathscr{R}}\sinh\left(l\sqrt{\frac{s_1}{a_L}}\right)}-\sqrt{\frac{s_1}{a_L}}-\frac{1}{R}\right] \quad [36]$$

is the transfer function of the bubble–cell system, s_1 = Laplace parameter, $\mathscr{R}(\Delta p)$ = image of the initial pressure perturbation, $l=\mathscr{R}-R_0$ and λ_L = thermal conductivity of the liquid.

As follows from [36], the asymptotic value of $G(s_1)$ for $s_1\to\infty$ ($\omega\to\infty, t\to 0$) is equal to

$$G(s_1)\approx\frac{\lambda_L T_0}{\rho_G L}\left(-\sqrt{\frac{s_1}{a_L}}-\frac{1}{R}\right). \quad [37]$$

Moving to the original of image [35], we will obtain, considering [37], an expression for the heat flux, which corresponds to [29].

The case $s_1\to 0$ ($t\to\infty, \omega\to 0$) determines the low-frequency asymptotes of $G(s_1)$ and q_L. Using the expansion of an exponent into a series, we will obtain, with an accuracy of $\sim s_1$, the following asymptotic value of $G(s_1)$:

$$G(s_1)=\frac{\lambda_L T_0}{\rho_G L}\frac{3\mathscr{R}+l^2}{2R^2}\cdot\frac{l}{a_L}\cdot s_1. \quad [38]$$

At $\epsilon\ll 1$ this expression assumes the form

$$G(s_1)=\frac{\lambda_L T_0}{\rho_G L}\frac{R}{3\epsilon_0 a_L}\cdot s_1. \quad [39]$$

Moving to the original, we obtain

$$q_L=\frac{C_{pL}\rho_L T_0 R}{3\epsilon_0\rho_G L}\frac{\partial p}{\partial t}. \quad [40]$$

Substituting the heat flux [40] into [28] and neglecting the dispersion and dissipative effects ($\beta=\eta=0$), we will obtain:

$$\frac{\partial^2 p}{\partial t^2}-\frac{c_0^2}{\left(1+\frac{c_0^2}{c_e^2}\right)}\frac{\partial^2 p}{\partial x^2}-\frac{\gamma+1}{2\gamma}\frac{c_0^2}{\left(1+\frac{c_0^2}{c_e^2}\right)}\frac{\partial^2}{\partial x^2}\left(\frac{\Delta p^2}{p_0}\right)=0. \quad [41]$$

Since $c_0^2/c_e^2\gg 1$ (for water: $p_0=1$ atm, $c_e\simeq 1$–3 m/s, $c_0\simeq 100$ m/s), then [41] can be written as

$$\frac{\partial^2 p}{\partial t^2}-c_e^2\frac{\partial^2 p}{\partial x^2}-\frac{\gamma+1}{2\gamma}c_e^2\frac{\partial^2}{\partial x^2}\left(\frac{\Delta p^2}{p_0}\right)=0. \quad [42]$$

Equation [42] describes a wave propagation at a thermodynamically equilibrium velocity c_e, and the linearized equation [42] coincides with the equilibrium model equation [19].

5. EVOLUTION OF A VAPOUR BUBBLE IN A PRESSURE WAVE

The experience of studying the wave dynamics of gas–liquid systems has shown that the propagation of perturbations, their structure and dynamics are largely determined by the dynamics of a solitary bubble. So the correct description of the interphase interaction processes, in particular, heat and mass transfer, determines the dynamics of the vapour cavity and, finally, provides a correct description of the wave structure and dynamics. The dynamics of a vapour bubble is governed by two mechanisms. First, if the intensity of phase transitions is low, then the behaviour of the bubble is governed by the so-called "inertial" mechanism, i.e. the behaviour of the bubble can be described by the Rayleigh equation [3]. If the variation in size of a vapour bubble is governed by the phase transition processes, then the "thermal regime" of bubble fluctuation is considered to occur. The crucial moment in the description of the interphase heat and mass transfer is the determination of the heat flux q_L with regard to the profile of pressure waves in the "thermal

regime" of bubble collapse or growth, as [29]. So special experiments studying the dynamics of a vapour bubble in the field of a pressure wave have been carried out to check this fundamental fact.

Synchronously with the pressure measurements in one of the pipe cross-sections, we took motion pictures at a speed of 8000 frame/s, which provided the correct correspondence of a pressure wave with the behaviour of a bubble therein. In the thermal regime, the bubble growth is determined by

$$q_L = L\rho_G \frac{dR}{dt}. \qquad [43]$$

It follows that

$$\frac{R}{R_0} = 1 \pm \frac{1}{R_0}\int_0^t \frac{q_L}{\rho_G L}\, dt. \qquad [44]$$

If we substitute q_L by [29] and integrate [44], then we will find the law of bubble radius variation with time, $R = R(t)$. It is easy to obtain some characteristic laws concerning the growth of a vapour bubble in the field of a wave. If the temperature T_s and pressure p vary in a stepwise manner [$T = T \cdot \chi(t)$, where $\chi(t)$ = Heaviside's function], then we obtain the following law of bubble radius variation:

$$\frac{R}{R_0} = 1 \pm \frac{2\lambda_L T_0 \Delta p}{R_0 (L\rho_G)^2 \sqrt{\pi a_L}} t^{1/2}. \qquad [45]$$

If the pressure drop is linear ($\Delta p = bt$), then we have the following relation:

$$\frac{R}{R_0} = 1 \pm \frac{4\lambda_L T_0 b}{3R_0 (L\rho_G)^2 \sqrt{\pi a_L}} t^{3/2}. \qquad [46]$$

Thus the analysis shows that, depending on the profile of a pressure wave, the bubble growth law changes. The most frequently used bubble growth law $R \sim \sqrt{t}$ is valid for stepwise loads only.

Let us refer to the results of the experiment. Figure 3 shows that in low-intensity waves (a, b) a bubble generally preserves its original form during its growth and collapse. If the intensity

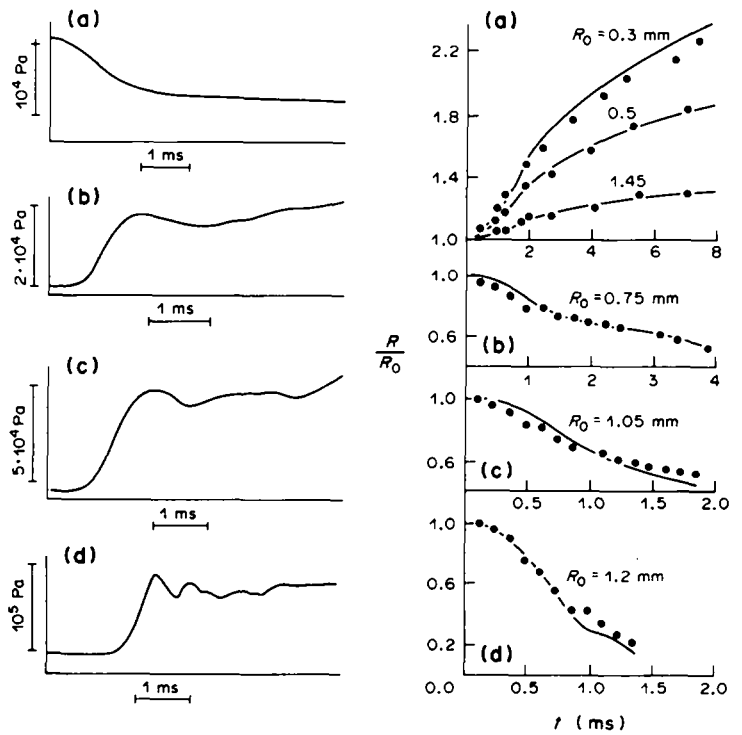

Figure 3. Growth (a) and collapse (b–d) of a vapour bubble in a pressure wave. ———, Calculation by [44].

increases (c, d), it deforms essentially and usually disintegrates at the end of the compression phase. In the case of a vapour–bubble mixture with $\epsilon_0 \simeq 0.01$ and an initial "stepwise" perturbation with the intensity $\Delta p = 10^5$ Pa turns, as it passes in the medium, into a wave with a characteristic "sharp" pulse (d), whose amplitude is 2.6 times as high as the intensity of the incident wave. The formation of the pulse seems to the connected with the decay and with the subsequent collapse of vapour bubbles which occurs practically at the leading wave edge for the given amplitude of the pressure wave.

The leading edge of the pressure drop and rise in the above experiments can be approximated as a first approximation by the linear dependence $\Delta p \sim bt$. Then it follows from [46] that in this section the bubble radius variation law can be described by the dependence $R \sim t^{3/2}$, whereas in the case of the horizontal section the regularity turns into $R \sim t^{1/2}$. Figure 4 compares the experimental data on bubble growth with the results obtained using both [46], [45] at the respective section of the pressure dependence, and [44] with the full wave shape taken into account.

Satisfactory agreement between calculation and experiment is attained while using the factor $\sqrt{3}$ in the addends of formulae [45] and [46]. In this case [45] at $R_0 = 0$ takes the form of the known solution (Plesset & Zwick 1954) for bubble growth from a micronucleus, which takes into account sphericity and mobility of the boundary.

Thus the experiments have shown that the dynamics of a vapour bubble is susceptible to the wave profile and that to develop a model of wave propagation in a liquid with vapour bubbles, the suggested flow describes the mass transfer process in the form of [29] sufficiently well.

6. ACOUSTICS AND LINEAR WAVES IN A VAPOUR–LIQUID MEDIUM

Let us consider a pressure perturbation as a harmonic wave with frequency ω and wavenumber k,

$$\Delta p = \Delta p_0 \exp(i\omega t - ikx);$$

and using [35] and [36] we will determine for this perturbation the heat flux on the interphase boundary:

$$q_L = G(i\omega)\Delta p_0 \exp(i\omega t). \qquad [47]$$

Substituting q_L into [28], we will obtain the following dispersive relation (Orenbakh & Shreiber 1986):

$$k^2 = \frac{\omega^2}{c_0^2} \frac{\left[1 - \dfrac{i}{\omega} \dfrac{3\gamma p_0}{r\rho_G L} G(i\omega)\right]}{\left(1 - \dfrac{2\beta\omega^2}{c_0^2}\right)}. \qquad [48]$$

The general form for the dependence of the phase sound velocity in a vapour–liquid medium on frequency is given in figure 5. The asymptotes of the dependence $c = c(\omega)$ at $\omega \to 0$ are also given. In this case

$$k^2 = \frac{\omega^2}{c_0^2}\left[1 - \frac{i3\gamma p_0}{\omega R \rho_G L} G(i\omega)\right] \qquad [49]$$

and the phase velocity tends to the equilibrium value c_e [18]. Earlier models (Mecredy & Hamilton 1972; Ardron & Duffey 1979; Nakoryakov *et al.* 1984b) yielded $c \to 0$ at $\omega \to 0$.

Analysis of the dispersive curve shows that in the case of a vapour–water mixture at $p_0 = 10^5$ Pa, $\epsilon_0 = 1\%$, there exists a thermodynamic equilibrium in the medium for a perturbation with $\omega \sim 0.1$ Hz. Typically, in real experiments the duration of perturbations ranged from 10^{-2} to 10^{-3} s. Therefore, signals propagating with equilibrium speed c_e have never been registered in experiments.

The dispersion law [48] can be assumed as a basis for predicting the dynamics of linear waves. The structure of linear waves can be calculated using the discrete Fourier transform and its numerical realization as an FFT algorithm. Expanding an initial perturbation into a discrete

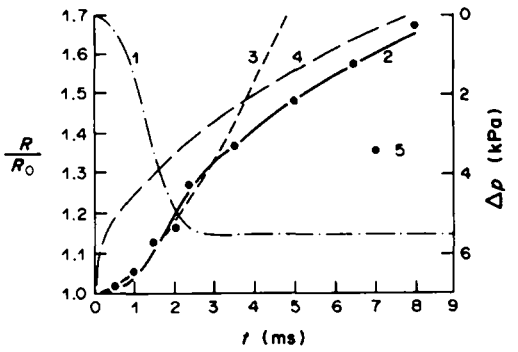

Figure 4. Comparison of experimental data on bubble growth with calculation. 1, Rarefaction wave profile; 2, calculation by [44]; 3, calculation by [46]; 4, calculation [45]; 5, experiment.

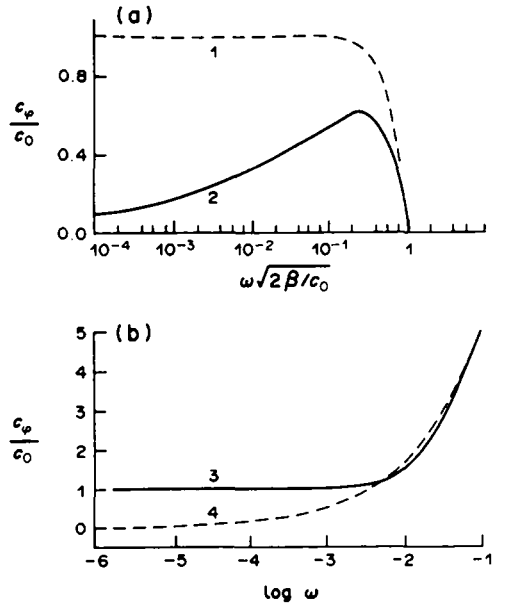

Figure 5. Dispersion of sound velocity in a liquid with vapour bubbles. (a) High frequencies, water—$p_0 = 10^5$ Pa, $R_0 = 10^{-3}$ m; 1, gas bubbles; 2, vapour bubbles; $T_0 = 373$ K. (b) Low frequencies; 3, calculation by [48]; 4, calculations by Ardron & Duffey (1979) and Nakoryakov *et al.* (1984b).

Fourier series and then, at a certain distance, "collecting" the harmonics into a signal again, one can restore the structure of the dispersion-transformed signal.

The formula for expansion of a linear wave into a finite sum of simple waves,

$$p(x, t) = \sum_{n=0}^{l-1} Z_n \exp(i\omega_n t - ik_n x), \qquad [50]$$

coincides at $x = 0$ with the reverse Fourier transform formula:

$$p_m = \sum_{n=0}^{l-1} Z_n \exp\left(\frac{i2\pi mn}{l}\right) \qquad [51]$$

if $p_m = p(0, m\Delta t)$, $\omega_n = 2\pi n/l\Delta t$, $t = m\,\Delta t$ = sampling rate, $T = l\Delta t$ = time interval, $m = 0, 1, \ldots, l-1$. So, if the boundary condition $p(0, m\Delta t)$ is known, then the factors Z_n in [50] can be found as follows:

$$Z_n = \sum_{n=0}^{l-1} p_m \exp\left(\frac{-i2\pi mn}{l}\right). \qquad [52]$$

For the fixed coordinate $x = x_0$, [50] is converted into

$$p(x_0, t) = \sum_{n=1}^{l-1} V_n \exp(i\omega_n t), \qquad [53]$$

where the expansion factors V_n are equal to

$$V_n = Z_n \exp(-ik_n x_0). \qquad [54]$$

Substituting the dispersion law $k = k(\omega_n)$ into [54], we can find the factors V_n for a given x and then carry out the reverse Fourier transform procedure to obtain the value of the functions $p_m = (x_0, m\Delta t)$. In the calculations it should be considered that $T_{\min} = x_{\max}/c_{\max}$ and $T_{\max} = x_{\max}/c_{\min}$.

The evolution of waves in a bubble vapour–liquid medium is shown in figure 6.

As can be seen, the formation of a wave and its propagation are strongly affected by the intensity of the interphase heat transfer. Here $\theta = 3\gamma p_0/R_0\rho_2 L$ is the factor of $\partial q_L/\partial t$ in [28]. The existence

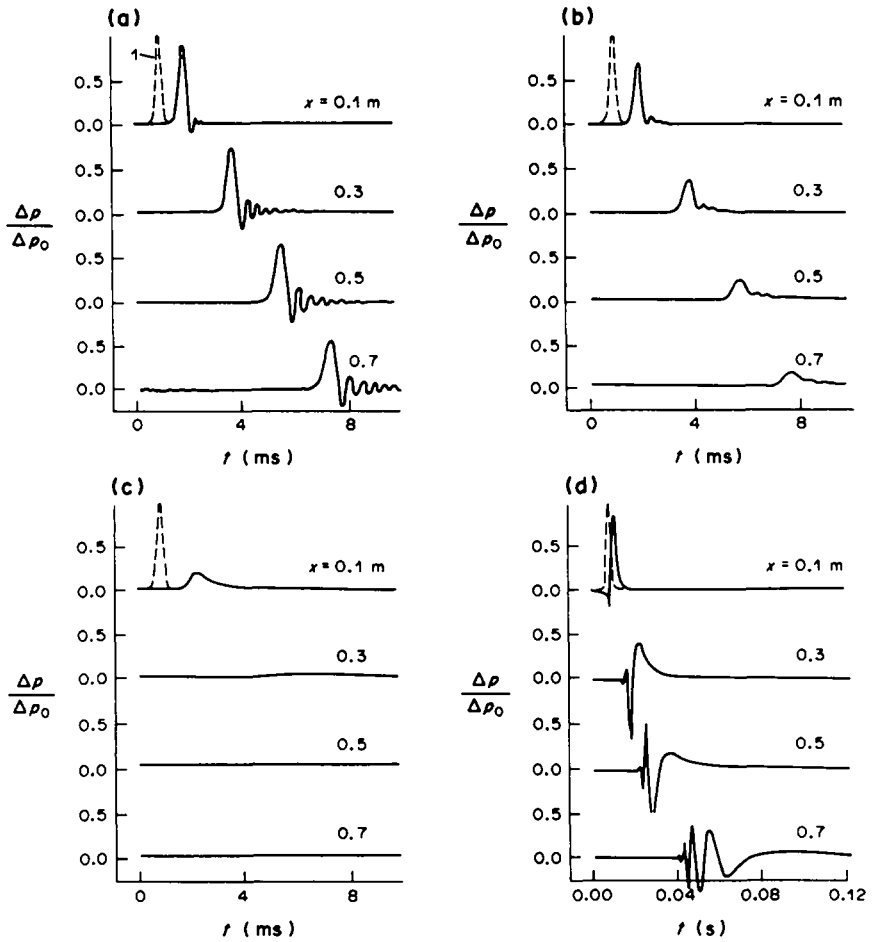

Figure 6. Evolution of a linear perturbation. 1, Initial wave $\beta = 4 \cdot 10^{-6}\,\mathrm{m}^2$. $c_0 = 113$ m/s; (a) $\theta = 5 \cdot 10^{-4}\,\mathrm{m}^{-1}$; (b) $\theta = 5.10^{-3}\,\mathrm{m}^{-1}$; (c) $\theta = 5 \cdot 10^{-2}\,\mathrm{m}^{-1}$. $a = 0.1\,\mathrm{m}^{-1}$.

of the sound velocity thermal dispersion should lead, as seems to be the case, to the appearance of a high-frequency precursor. To demonstrate the existence of the thermal dispersion, one may artificially assume that $\mathrm{Im}(k) = 0$. In this case [figure 6(d)] we actually obtain oscillations leading the basic low-frequency signal.

7. PROPAGATION OF NONLINEAR WAVES IN A LIQUID WITH VAPOUR BUBBLES

Equation [28], describing the propagation of nonlinear waves, can be formally factorized, i.e. waves going "to the right" or "to the left" can be singled out. Using the mode of nonlinear wave dynamics (Karpman 1973), we can obtain an equation for a wave running to one side:

$$\frac{\partial p}{\partial t} + c_0 \frac{\partial p}{\partial x} + \frac{\gamma + 1}{2\gamma} c_0 \frac{\Delta p}{p_0} \frac{\partial p}{\partial x} - \eta \frac{\partial^2 p}{\partial x^2} + \beta c_0 \frac{\partial^3 p}{\partial x^3} = \frac{3}{2} \frac{\gamma p_0}{R_0 \rho_G L} q_L. \qquad [55]$$

Analysis of the obtained dispersive relations has shown that q_L can be taken in the form [29]. Then [55] will assume the form

$$\frac{\partial p}{\partial t} + c_0 \frac{\partial p}{\partial x} + \frac{\gamma + 1}{2\gamma} c_0 \Delta p \frac{\partial p}{\partial x} - \eta \frac{\partial^2 p}{\partial x^2} + \beta c_0 \frac{\partial^3 p}{\partial x^3} = -\frac{m\sqrt{a_L}}{2\sqrt{\pi R_0^2}} \int_0^t \frac{\partial p / \partial t'}{\sqrt{t - t'}} \mathrm{d}t' \qquad [56]$$

where

$$m = \frac{3\gamma p_0 \rho_L c_{p_L} \left(\frac{dT}{dp}\right)_s}{\rho_G L}.$$

By employing similarity theory methods it is possible to obtain from [56] the minimal number of similarity criteria that are needed to determine the evolution of the wave process in vapour–liquid media. For this purpose, we reduce [56] to a dimensionless form using the initial perturbation parameters: the amplitude Δp_0, the duration l_0 (for perturbations of finite duration) and the quantity c_0 as the characteristic velocity. The model equation [56] will take the form (Nakoryakov *et al.* 1982):

$$\frac{\partial p^*}{\partial \tau} + \frac{\partial p^*}{\partial \xi} + Mp^* \frac{\partial p^*}{\partial \xi} + \frac{M}{\mathrm{Re}} \frac{\partial^2 p^*}{\partial \xi^2} + \frac{M}{\sigma^2} \frac{\partial^3 p^*}{\partial \xi^3} = -WM^{1/2} \int_0^\tau \frac{\frac{\partial p^*}{\partial \tau}}{\sqrt{\tau - \tau^1}} d\tau', \qquad [57]$$

where

$$\tau = \frac{c_0 t}{l_0}; \quad \xi = \frac{x}{l_0}; \quad p^* = \frac{\Delta p}{\Delta p_0}.$$

It follows from [57] that the dynamics of pressure perturbations in a vapour–liquid medium is characterized by the following criteria.

- For a perturbation of finite duration:

$$\sigma = l_0 \left[\frac{(\gamma + 1)\Delta p_0}{2\gamma p_0 \beta}\right]^{1/2},$$

which determines the contribution of nonlinear effects (as compared with dispersive ones) into the wave profile distortion;

$$W = m \left[\frac{\gamma p_0 a_L l_0}{2\pi R_0^2 c_0 \Delta p_0 (\gamma + 1)}\right]^{1/2},$$

which characterizes the relative role in the interphase heat transfer and nonlinear effects;

$$\mathrm{Re} = \frac{(\gamma + 1) c_0 \Delta p_0 l_0}{2\gamma p_0 \eta},$$

which is the Reynolds number, characterizing the dissipation in a medium without phase transitions.

- For shock wave-type perturbations:

$$W_* = W\sigma^{-1/2} = m \left[\frac{a_L \sqrt{\beta u_0}}{4\pi R_0^2 u_0 \sqrt{c_0}}\right]^{1/2},$$

which determines the effect of the phase transition and nonlinear twisting of a wave;

$$M = \frac{u_0}{c_0} = \frac{(\gamma + 1)\Delta p_0}{2\gamma p_0},$$

which is the Mach number.

At high values of W (or W_*) the determining effect on the evolution of waves should be exerted by a phase transition; when $W \to 0$, it is the dependence of the wave behaviour on nonlinear and inertial effects which should become essential. This suggests the possibility of the existence, in a bubble medium with phase transitions, of diverse wave patterns: wave packets, solitons, shock waves of monotonous or oscillatory structure.

In the case of a weak influence of phase transitions (W_*, $W \to 0$), the necessity arises to allow for other dissipative effects (viscous friction in oscillations of bubbles, acoustic losses due to liquid compressibility). These effects can be accounted for within the framework of the model using the "effective" viscosity η, then dissipation is characterized by the Reynolds number Re.

At $\mathrm{Re}^{-1} > W$ (for shock waves $\sigma/\mathrm{Re} > W^*$), the determining dissipative mechanism in the wave evolution becomes that associated with viscous losses. However, one should note the following: the actual range reached by the values of W, e.g. at $R_0 \sim 1$ mm and $\epsilon_0 \sim 10^{-2}$ for the majority of vapour–liquid media (liquid metals, vapour–water media, cryogenic liquids) is of the order of 50–10^{-4}, whereas the quantity Re^{-1} for these conditions varies from 10^{-3} to 10^{-4}.

The similarity criteria were assumed as a basis for planning a program of experiments and their subsequent processing. It is necessary to choose the parameters of a boiling flow and the characteristics of an initial perturbation such that a much wider range of variation of the criteria W and σ (M and W_*) would be available. For this purpose, an effective method of investigation is the shock-tube method, allowing one not only to fix the structural parameters of a vapour–liquid medium and vary the vapour phase dispersion and concentration degree, but also to obtain a wide range of the initial characteristics such as duration and intensity. The analysis of experimental data on the basis of the above similarity criteria has revealed a number of regions of W, σ and M where the character of the evolution of the waves differs.

Let the region $W_* \gtrsim 1$ be called the "thermal" regime. The essential feature here is the dominating effect of the interphase heat transfer. It has been found in experiments that nonlinear and inertial effects do not take part in the formation of waves at all [figure 7(a)]. This allows one to consider the evolution of waves on the basis of the linear equation which follows from [57]:

$$\frac{\partial p^*}{\partial \tau} + \frac{\partial p^*}{\partial \xi} = -W \cdot M^{1/2} \int_0^\tau \frac{\dfrac{\partial p^*}{\partial t'}}{\sqrt{\tau - \tau'}}. \qquad [58]$$

The solutions of [58] for various initial perturbations can be obtained by the Laplace transform. For example, for a stepwise initial perturbation the solution of [58] can be written as (Nakoryakov & Shreiber 1979):

$$\frac{\Delta p}{\Delta p_0} = \mathrm{erfc}\left[\frac{mx}{16\, c_0 \sqrt{\left(\dfrac{R_0^2}{a_L}\right)\left(\dfrac{t-x}{c_0}\right)}}\right]. \qquad [59]$$

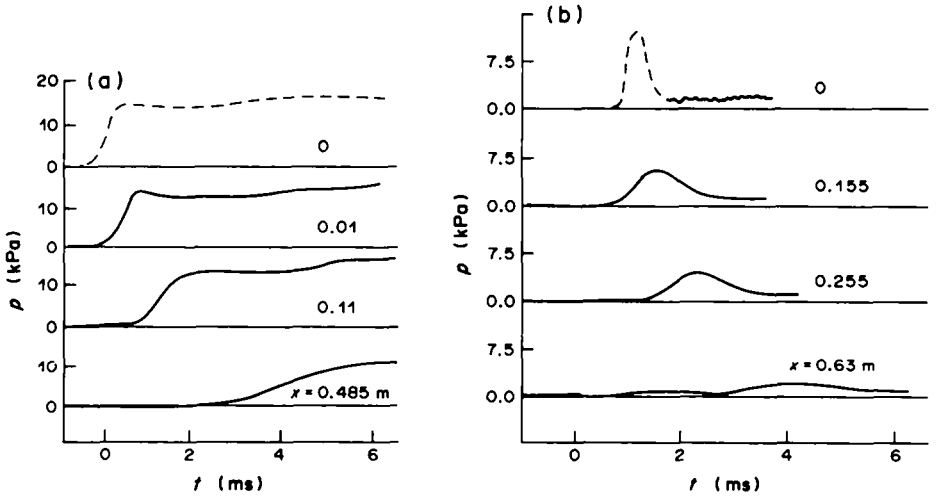

Figure 7. Evolution of waves in the thermal regime. Water, $p_0 = 0.19$ MPa, $\epsilon_0 = 0.01$, $R_0 = 1.5$ mm. (a) Shock wave, $M = 0.07$, $W_* = 0.72$. (b) Impulse perturbation, $M = 0.05$, $\sigma = 2.4$, $W_* = 1.36$.

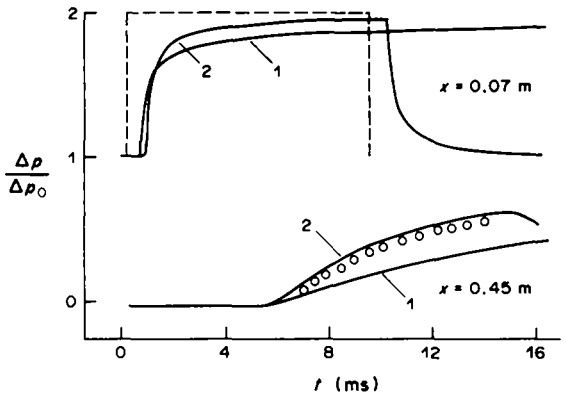

Figure 8. Linear waves in water with vapour bubbles. $p_0 = 0.1$ MPa, $c_0 = 100$ m/s, $R_0 = 1$ mm, $\epsilon_0 = 0.01$; 1, Calculation by [59]; 2, calculation by [28], $\theta = 0.222$ m^{-1}; ○, experiment.

However, the comparison of the calculation using this formula with the respective experiment points to a certain discrepancy in the data (figure 8). One can understand the reason by analysing the solutions of the complete equation [28], where q_L is determined by [31]. This equation has the form of the Boussinesq equation with the integral r.h.s. and describes waves propagating to both sides. An example for numerical modelling of an initial perturbation on the basis of [28] is shown in figure 9. The calculations have been carried out using the above FFT transform procedure. One can see that if the interphase heat transfer is intensive enough ($\theta = 0.02$), the initial pulse has no chance to divide into two perturbations and evolves as a whole. Therefore, under such conditions, the conversion to the evolution equation, describing the wave moving on one side is invalid, and the wave propagation should be calculated on the basis of the complete equation [28]. In this case the agreement between the calculated and experimental result is rather satisfactory (figure 8, line 2).

A typical picture of the progress of a finite-duration wave process is shown in figure 7(b). A substantial spread and decay of the pressure wave amplitude leads to the virtual disappearance of the perturbation already at the distance $x \sim 1$ m. Such a wave evolution in this regime is observed up to an incident perturbation intensity $M \sim 0.5$. With a further increase in the incident perturbation intensity, the waves in a vapour–liquid medium strengthen—just as during their reflection from a wall, and as in a direct wave (figure 10). The reported elements on the amplification of waves have not been described theoretically as yet. This requires more detailed theoretical and experimental studies on the formation of waves and on the behaviour of a vapour–liquid medium therein. In the present paper such tests are presented only as an illustration

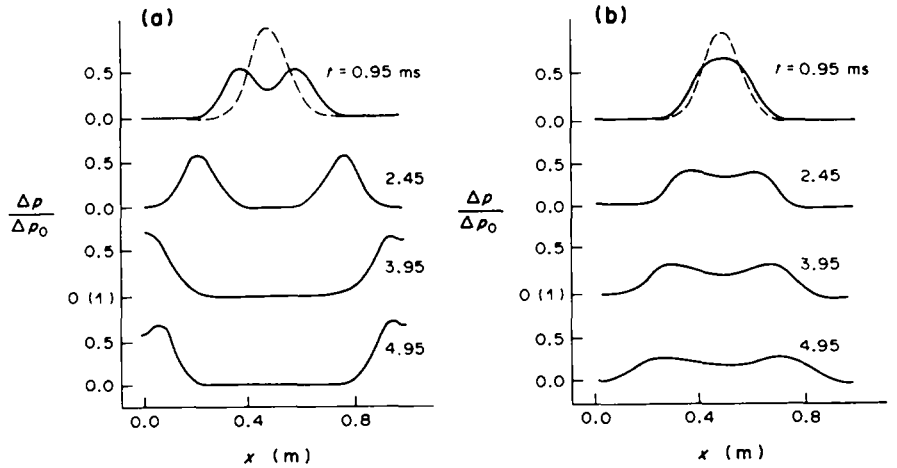

Figure 9. Evolution of a finite signal for different intensities of interphase heat transfer. (a) $\theta = 0.002$ m^{-1}; (b) $\theta = 0.02$ m^{-1}.

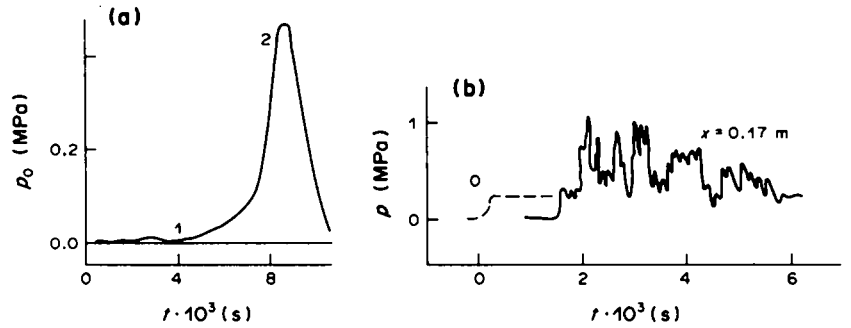

Figure 10. Amplification of waves in a vapour–liquid medium. (a) Reflection from the wall (1, incident wave; 2, reflected wave); (b) propagation of a wave. (a) Water—$p_0 = 0.1$ MPa, $\epsilon_0 = 0.02$, $R_0 = 1.5$ mm; (b) Freon-21—$p_0 = 0.17$ MPa, $\epsilon_0 = 0.01$. $R_0 = 1.2$ mm.

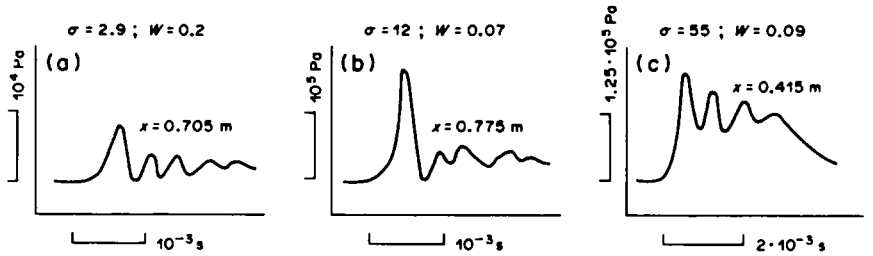

Figure 11. The structure of perturbations in the inertial regime; $\epsilon_0 = 0.01$. (a, b) Freon-12 $p_0 = 1.3$ MPa, $R_0 = 1$ mm; (c) Freon-21—$p_0 = 0.2$ MPa, $R_0 = 1.2$ mm.

of the application range for the derived criteria and model equation [57] in the analysis of the wave dynamics.

The region $W_* < 0.1$ is the "inertial" regime. In this region the character of the evolution of finite-length pressure waves depends on the number σ. There exists a value σ_*, determined by the type of initial perturbation only, that at $\sigma < \sigma_*$ a wave packet develops in a vapour–liquid medium [figure 11(a)], whereas at $\sigma \geqslant \sigma_*$ solitary waves develop [figure 11(b)]. In this regime, there are shock waves with two types of thin structure: monotonous ($M < 0.3$) and oscillatory ($M > 0.3$) (figure 12), with the parameters (shape, steepness of the leading edge, maximum pressure in oscillation, velocity) being preserved at large distances. The different character of the wave process revealed in the experiments is in complete agreement with the results of the theoretical analysis of

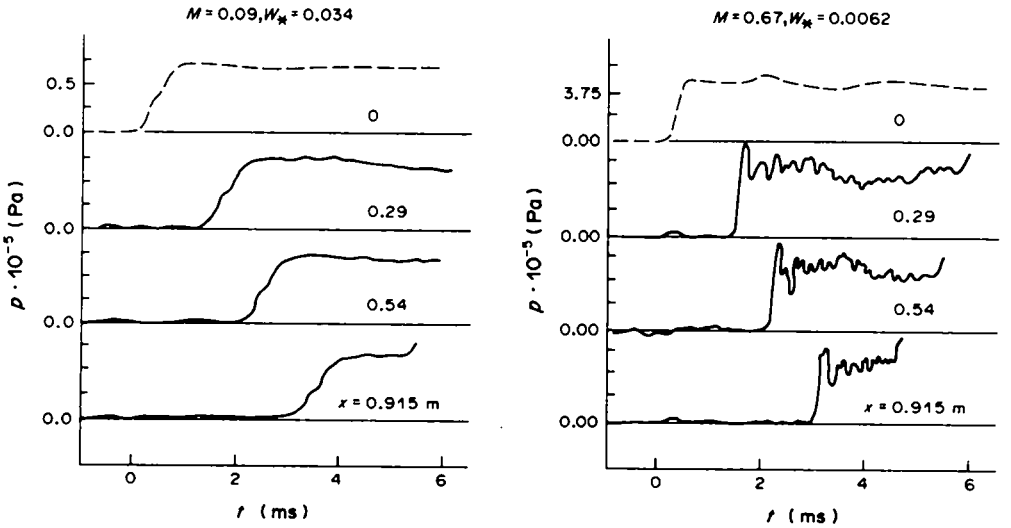

Figure 12. Shock waves in a liquid with vapour bubbles. Freon-12—$p_0 = 0.7$ MPa, $\epsilon_0 = 0.01$, $R_0 = 1.3$ mm.

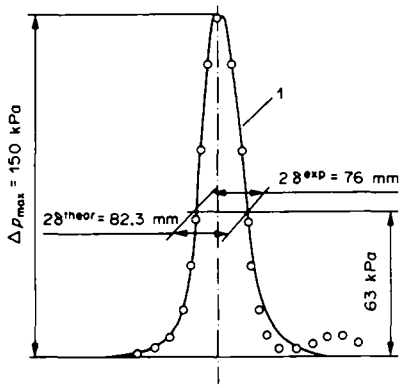

Figure 13. Wave form as compared to the form of a soliton. Experiment: Freon-12—$p_0 = 1.3$ mPa, $\epsilon_0 = 0.01$, $R_0 = 1$ mm, $\Delta p_0 = 190$ kPa, $x = 0.77$ m. 1, Calculation by [60].

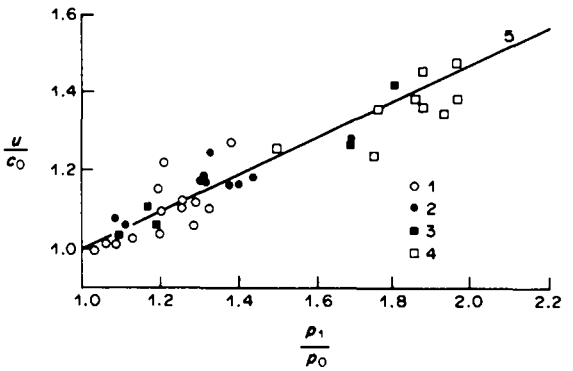

Figure 14. Velocity of shock waves in a vapour–liquid medium. $p_0 = 0.5$ mPa, $R_0 = 1.4$ mm. 1, $\epsilon_0 = 0.01$; 2, $\epsilon_0 = 0.018$, Freon-12—$p_0 = 0.7$ mPa, $R_0 = 1.3$ mm; 3, $\epsilon_0 = 0.008$; 4, $\epsilon_0 = 0.015$; 5, calculation.

the solution to the model equation [57] for $W_* \to 0$. Really, at $W_* = 0$ the model equation turns into the well-known Burgers–Korteweg-de Vries equation, admitting, for example, solutions in the form of a solitary wave (i.e. a soliton):

$$\Delta p(x) = \Delta p_{max} \operatorname{sech}^2\left(\frac{x}{\delta}\right)$$

$$\delta = \left[\frac{4\gamma}{(\gamma+1)}\right]^{1/2}\left(\frac{p_0}{\Delta p_{max}}\right)^{1/2}\frac{R_0}{\epsilon_0^{1/2}}. \qquad [60]$$

The calculation by [60] and the shape of the wave determined experimentally are presented in figure 13.

Figure 14 shows the velocity of the propagation of perturbations in a vapour–liquid medium at $W_* < 0.1$. As follows from the analysis of the similarity numbers and model equation [57], the wave packets move with the frozen sound velocity c_0, the velocities-u of solitary waves and shock waves are, respectively, governed by the relations:

$$\frac{u}{c_0} = \frac{1+(\gamma+1)\Delta p_{max}}{6\gamma p_0} \quad \text{and} \quad -\frac{u}{c_0} = \frac{1+(\gamma+1)\Delta p_0}{4\gamma p_0}.$$

The transition region is $0.1 \leqslant W_* < 1$. Above we have considered the main laws governing the progress of wave processes in two limiting cases in which the propagation of perturbations can be successfully calculated from simple analytical expressions. We will now consider some regularities in the behaviour of the waves when they pass from the inertial regime to the thermal one.

The data on the wave propagation with $\sigma \sim 9$ (a soliton in the "inertial" regime), presented in figures 15 and 16, clearly confirm the following fact. As the values of W_* increase, from being extremely small, the character of the evolution of waves varies—the interphase heat transfer begins to influence the process to a greater degree. Although at small distances, with the growth of W_* the perturbation shape still corresponds to the shape of the soliton, this formation is no longer a stable one. In the course of further evolution, the initially balanced influence of the inertial and nonlinear effects is replaced by the dominating influence of interphase heat transfer. The initial perturbation is transformed into a wave with markedly larger spatial–temporal scales than those of the soliton with the same amplitude. A further increase in W_* leads to the perturbation undergoing evolution in the same way as in the "thermal" regime considered above. An analogous situation is also observed at further values of σ. Such a solitary soliton, a multi-soliton perturbation and a wave packet, which are stable formations in the case where $W_* \to 0$, gradually degenerate, with an increase in W_*, into a smooth bell-shaped wave of the "thermal" regime and the faster they degenerate, the higher the value of W_* and the smaller the value of σ.

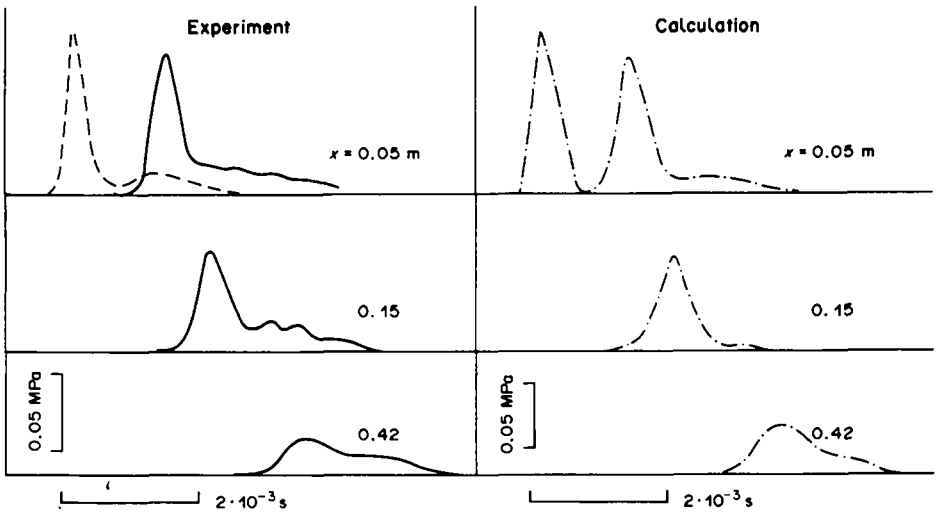

Figure 15. Comparison of experiment with calculation by the model equation [56]. Water—$p_0 = 0.5$ MPa, $\epsilon_0 = 0.015$, $R_0 = 1.4$ mm, $\sigma = 9.1$, $W = 0.38$.

The degree of perturbation attenuation is different at different values of W_*. It is well-illustrated in figure 16 where a change in the wave amplitude with $\sigma \sim \sigma_*$ is shown. The observed difference in the attenuation laws is, first of all, connected with the change in the interphase heat transfer contribution to the formation and motion of perturbations. Two limiting calculated lines 1 and 2 in figure 16 show, respectively, the attenuation of a soliton in a bubble system with the frozen phase transition (calculation by [57] at $W_* = 0$) and the attenuation of a perturbation due to the interphase heat transfer alone (calculation by [58]). One can clearly see that in a vapour–liquid medium the initial perturbation, which has covered a distance of approx. 1 m, can either disappear completely (i.e. reduce its amplitude by more than a factor of 100) or remain practically unchanged (i.e. reduce its amplitude only by a factor of 1.25).

Analytical inspection of the unsteady wave process progress within the range $0.01 < W_* < 1$ is extremely difficult, and in this case a numerical solution of the model equation or the complete set of equations [56] or [57] is more expedient. The accuracy of the numerical integration of [57] has been tested by comparison of the results both with well-known numerical solutions of the KDV equation (Berezin 1977) and with analytical solutions of [58]. Also, the numerical solution of the linearized equation [56] was compared with that solved using the FFT technique on the basis of the determined dispersive equation [49].

The values of the factors in [57] were calculated for the initial conditions of the experiments, and the solutions of the equations were derived at distances x corresponding to the coordinates of the probes. Figure 17 shows the results of the "shock-wave"-type calculations. Figure 18 shows a calculation of the finite-length wave structure which is compared with the results of the experiments.

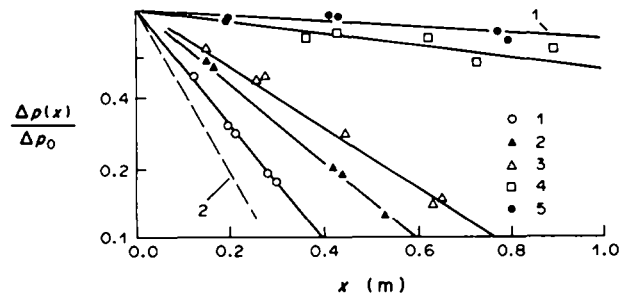

Figure 16. Attenuation of a solitary wave in a vapour–liquid medium. 1, Water—$p_0 = 0.13$ MPa, $\epsilon_0 = 0.01$. $R_0 = 1.5$ mm; $M = 0.18$, $\sigma = 9$, $W = 1.5$; 2, water—0.5 0.015 1.4 0.2 9 0.35; 3, Freon-21—0.19 0.01 1.2 0.3 12 0.25; 4, Freon-12—0.66 0.015 1.3 0.25 11 0.06; 5, Freon-12—1.3 0.01 1 0.13 9 0.07.

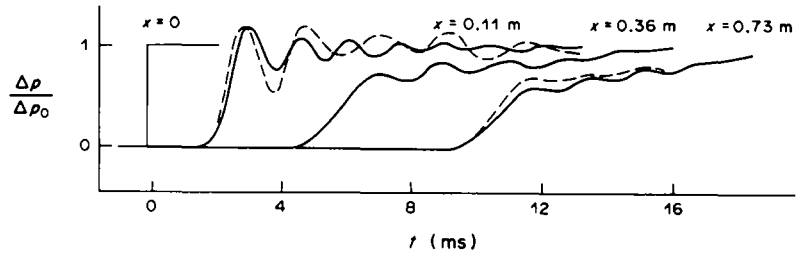

Figure 17. Evolution of a "step-type" initial perturbation.

8. SHOCK WAVES

A very important problem of the gas dynamics of a vapour–liquid medium concerns the existence of shock waves.

As is known, the formation of shock waves is connected with the competition between two mechanisms—nonlinearity and dissipation. The corresponding similarity criterion characterizing the contribution of these mechanisms to the wave evolution in a bubble vapour–liquid medium can be obtained from [56] by comparing the integral and the nonlinear sides.

At large values of W_* ($W_* > 1$) the interphase heat transfer is dominating in the wave evolution, and originally steep perturbations should transform into gently sloping ones.

In this case, the leading edge of a wave widens considerably as it propagates. Its length, found from the maximum inclination region, is comparable with the distance covered by the wave. To compensate for the severe flattening of the leading edge by increasing, within certain limits, the intensity of the original perturbation turns out to be impossible—the evolution of a wave with a large Mach number occurs analogously. The velocity of such gently sloping waves corresponds to the value c_0.

If one changes the thermophysical properties of the medium so that the value of the criterion W_* decreases, then the flattening of the leading edge becomes slower. The wave structure begins to depend on the intensity. If the intensity is weak ($M < 0.3$), the wave form is always monotonous; at $M > 0.3$, the inertial effects form an oscillating structure in the starting section (figure 19). A finite-width jump occurs in the medium. Its existence is, however, limited to small distances. Already, the oscillations degenerate at 0.5 m from the entrance of a perturbation into the medium, and at large distances the influence of nonlinearity disappears too. The wave profile is formed mainly by the interphase heat transfer.

The duration of the existence of the shock-profile essentially increases with subsequently increasing W_*. At $W_* \sim 10^{-2}$, quasi-stationary shock waves were present over the entire length of the working section. Depending on the intensity of a wave, either the monotonous or the oscillatory wave structure (figure 12) was realized. The velocity of waves depends on their amplitude.

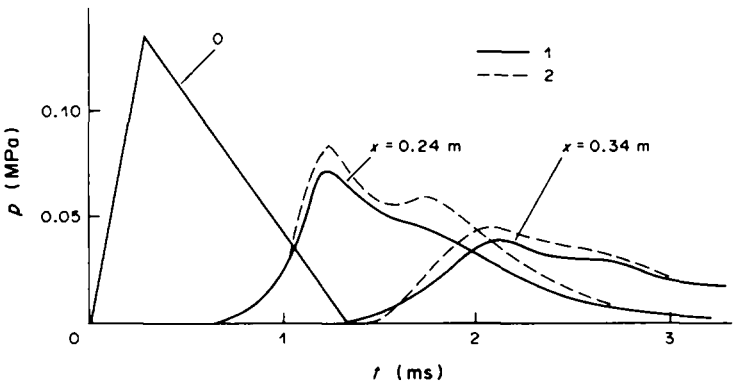

Figure 18. Evolution of a wave with $\sigma > \sigma_*$. 1, Calculation by [56]. Water—$p_0 = 0.18$ MPa, $\epsilon_0 = 0.01$, $R_0 = 1.5$ mm, $\sigma = 26.5$, $W = 0.67$.

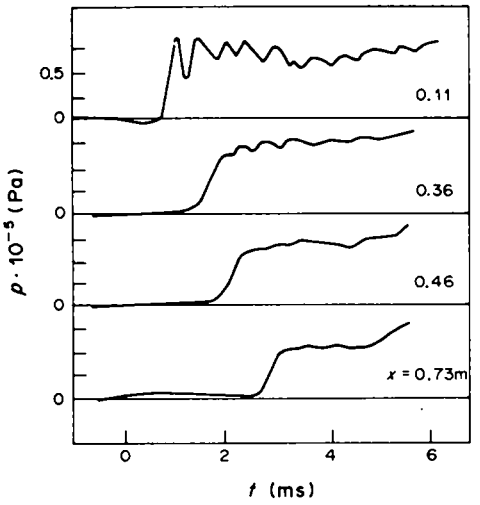

Figure 19. Degradation of a shock wave. Experiment: Freon-21—$p_0 = 0.185$ MPa, $\epsilon_0 = 0.01$, $R_0 = 1.2$ mm, $\Delta p_0 = 0.69\ 10^{5}$ Pa.

The time of existence of a shock wave t^* can be estimated assuming that during this time the equilibrium between the nonlinear effects and dissipation still exists. Let us assume that the structure of the wave front is close to a "step". In this case the heat flux q_L can be written as

$$q_L = -\frac{\rho_L c_{p_L}}{\sqrt{\frac{\pi t^*}{a_L}}\left(\frac{dT}{dp}\right)_s}\Delta p. \qquad [61]$$

Substituting [16] into [28] and making this equation dimensionless with respect to the characteristic time t^*, we find the following conditions for the existence of shock waves in the medium (Nakoryakov *et al.* 1984a):

$$t^* < \frac{\pi R_0^2}{4 a_L m^2}\left(\frac{\Delta p_0}{p_0}\right)^2. \qquad [62]$$

The distance from the entrance of a perturbation into the medium x^*, at which a shock wave exists, can be estimated taking c_0 as the chartacteristic velocity.

The values of x^* for some vapour–liquid media ($\Delta p_0/p_0 = 0.3$) are: water, $p_0 = 0.1$ MPa, $T_0 = 100°C$, $x^* = 0.012$ m; water, $p_0 = 8.5$ MPa, $T_0 = 300°C$, $x^* = 13.6$ m; Freon-12, $p_0 = 0.66$ MPa, $T_0 = 25.4°C$, $x^* = 11$ m.

As can be seen, in a vapour–liquid medium existing at low pressures shock waves do not appear. Estimations in accordance with [62] show that a similar situation can also be observed for boiling liquid metal media. That is why Grolmes & Fauske (1968) did not discover that the velocity depends on the amplitude. On the contrary, in water boiling at high pressures shock waves can form, which is confirmed by the wave velocity data and experiments of Nakoryakov *et al.* (1982) and Sarkisov *et al.* (1981).

The results of the calculation by [62] for x^* are in good agreement with the experiments. As in the experiment shown in figure 7(a), no pressure jump is observed. Here $x^* = 5$ mm. For the conditions of the experiment shown in figure 19, $x^* = 0.38$ m, and at distances which are greater than this value the shock wave (as can be seen) degenerates. In the case shown in figure 12, $x^* = 20$ m. Here the parameters of the shock wave are the same along the entire length of the experimental setup.

The generalized plot given in figure 20 is an illustrative example showing the possible ways of evolution for initial shock waves in a boiling liquid. The wave profiles are given here for the time $t \sim 5 \cdot 10^{-3}$ s. Using figure 20, the similarity criteria, W_* and M, and condition [62], one can

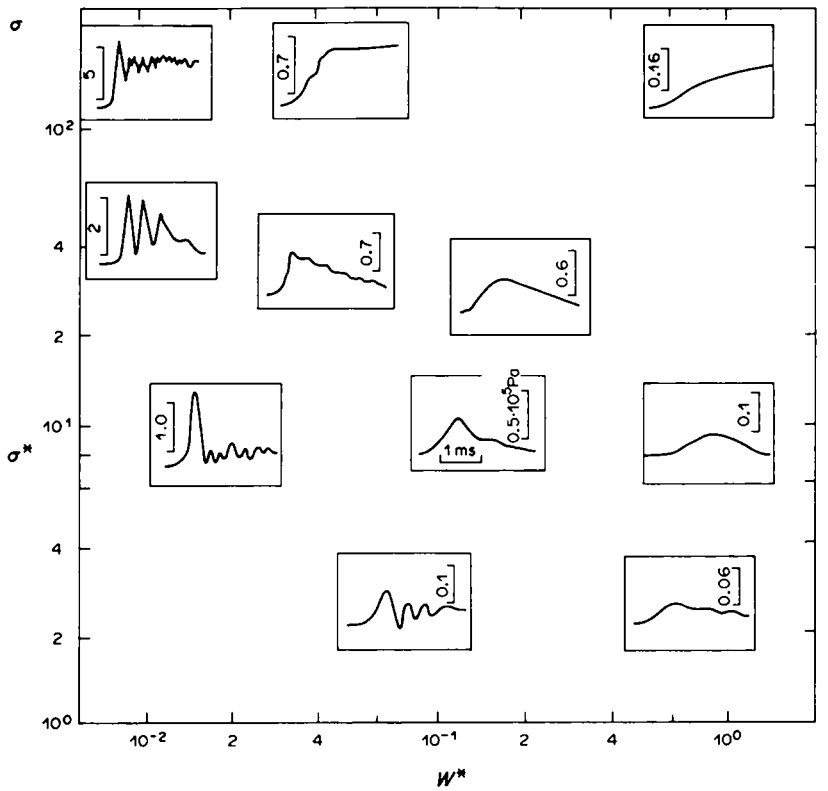

Figure 20. Generalized picture of a pressure wave formation in a vapour–liquid medium with bubbles structure.

successfully predict the dynamics of finite-amplitude pressure jumps in any vapour–liquid media (cryogenic liquids, liquid metals, molten organic solid substances etc.).

For sodium, boiling at $p = 0.1$ MPa, with the medium parameters $\epsilon_0 = 0.01$, $R_0 = 1.5$ mm and an initial perturbation $\Delta p_0/p_0 \sim 0.4$, the value of the criterion $W_* \sim 15$. As we have already seen, for such values of W_* the pressure pulses in the medium will be considerably diffused and attenuated and the leading edge of the initial shock wave will become much flatter. On the contrary, in the case of hydrogen, boiling under the same initial conditions, there are very small values of W_* ($W_* \sim 6 \cdot 10^{-4}$). This means that the wave dynamics of such a medium will be governed in the main by the inertial and nonlinear effects. Low values of W_* ($W_* \sim 10^{-3}$) can also be obtained for a vapour–water mixture at $p_0 \sim 3$ MPa.

REFERENCES

ARDRON, K. H. & DUFFEY, R. B. 1979 Acoustic wave propagation in a flowing liquid–vapour mixture. *Int. J. Multiphase Flow* **4**, 303–322.

AVDONIN, V. I. & NOVIKOV, I. I. 1960 Sound velocity on vapour–liquid phase equilibrium curve. Sound velocity in saturated water vapour. *Zh. prikl. Mekh. tekh. Fiz.* **1**, 58–62.

BATCHELOW, G. 1968 Compression waves in a suspension of gas bubbles in a liquid. *Mekh. Sb. Inoctr. Statei* **3**, 67–84.

BEREZIN, YU. A *Numerical Study of Nonlinear Waves in Rarefied Plasma.* Nauka, Moskow.

DEICH, M. YE., FILIPOV, G. A. & STEKOLSHCHIKOV, YE. V. 1964 Sound velocity in two-phase media. *Teploenergetika* **8**, 33–36.

FINCH, R. D. & NEPPIRAS, E. A. 1973 Vapour bubble dynamics. *J. acoust. Soc. Am.* **53**, 1402–1410.

GASENKO, V. G., NAKORYAKOV, V. E. & SHREIBER, I. R. 1977 Burgers–Korteweg–de Vries approximation in wave dynamics of gas–liquid systems. In *Nelineinye Volnovye Protsessy v dvukhfaznykh sredakh* (Edited by KUTATELADZE, S. S.), pp. 17–35. Institute of Thermophysics, Novosibirsk.

GROLMES, M. A. & FAUSKE, H. K. 1968 Comparison of the propagation characteristics of compression and rarefaction pressure pulses in two phase one component bubble flow. *Trans. Am. nucl. Soc.* **11,** 683–685.

KARPMAN, V. I. 1973 *Nonlinear Waves in Dispersing Media.* Nauka, Moskow.

KOGARKO, B. S. 1961 On one model of cavitating liquid. *Dokl. Akad. Nauk SSSR* **137,** 1331–1333.

KUTATELADZE, S. S., NAKORYAKOV, V. E. & POKUSAEV, B. G. 1979 Experimental investigation of wave processes in gas– and vapour–liquid media. In *Two-Phase Momentum Heat and Mass Transfer in Chemical Process & Energy Engineering*, Vol. 1, pp. 47–50. Hemisphere, New York.

KUZNETSOV, V. V., NAKORYAKOV, V. E., POKUSAEV, B. G. & SHREIBER, I. R. 1978 Propagation of perturbation in gas–liquid mixture. *J. Fluid Mech.* **85,** 85–96.

LANDAU, L. D. & LIFSHITS, YE. M 1953 *Mechanica Sploshnych Sred.* Gostekhizdat, Moskow.

MECREDY, R. C. & HAMILTON, L. J. 1972 The effects of nonequilibrium heat, mass and momentum transfer on two-phase sound speed. *Int. J. Heat Mass Transfer* **15,** 61–72.

NAKORYAKOV, V. E., SOBOLEV, V. V. & SHREIBER, I. R. 1972 Long-wave perturbations in gas–liquid mixture. *Izv. Akad. Nauk SSSR* **5,** 71–76.

NAKORYAKOV, V. E., SOBOLEV, V. V. & SHREIBER, I. R. 1975 Finite-amplitude waves in two-phase media. In *Volnovye Protsessy v Dvukhfaznykh Sistemakh* (Edited by KUTATELADZE S. S.), pp. 5–53. Institute of Thermophysics, Novosibirsk.

NAKORYAKOV, V. E. & SHREIBER, I. R. A model of perturbation propagation in vapour–liquid mixture. *Theploph. Vysokich Themper.* **17,** 798–803.

NAKORYAKOV, V. E., POKUSAEV, B. G., PRIBATURIN, N. A. & SHREIBER, I. R. 1982 Propagation of finite-amplitude pressure perturbations in a bubble vapour–liquid medium. *Zh. prikl. Mekh. tekh. Fiz.* **3,** 84–90.

NAKORYAKOV, V. E., POKUSAEV, B. G., PRIBATURIN, N. A. & SHREIBER, I. R. 1984a Shock waves in boiling liquid. *Int. Commun. Heat Mass Transfer* **11,** 55–62.

NAKORYAKOV, V. E., POKUSAEV, B. G., PRIBATURIN, N. A. & SHREIBER, I. R. 1984b Acoustics of a liquid with vapour bubbles. *Akust. Zh.* **30,** 808–812.

NIGMATULIN, R. I. 1978 *The Fundamentals of Heterogeneous Mechanics.* Nauka, Moskow.

NIGMATULIN, R. I. 1982 Mathematical modelling of a bubbly liquid motion and hydrodynamical effects in wave propagation phenomena. *Appl. scient. Res.* **38,** 267–289.

ORENBAKH, Z. M. & SHREIBER, I. R. 1986 Wave propagation in a liquid with phase transitions. *Akust. Zh.* **32,** 76–80.

POKUSAEV, B. G., KORABEL'NIKOV, A. V. & PRIBATURIN, N. A. 1981 Pressure waves in a liquid containing vapour bubbles. *Fluid Mech.–Soviet. Res.* **11,** 67–94.

PLESSET, M. S. & ZWICK, S. A. 1954 The growth of vapour bubbles in superheated liquids. *J. appl. Phys.* **25,** 493–500.

RADOVSKII, I. S. 1970 Sound velocity in two-phase vapour–liquid systems. *Zh. prikl. Mekh. tekh. Fiz.* **5,** 78–85.

SARKISOV, A. A., POPOV, I. A. & LUKYANOV, A. A. 1981 Boiling flow dynamics with shock perturbations. In *Teploobmen, Temperaturnyi Rezhim i Gidrodinamika pri Generatsii Para*, Nauka, pp. 39–48. Nauka, Leningrad.

SEMYONOV, N. I. & KOSTERIN, S. I. 1964 Results of studying sound velocities in moving gas–liquid mixtures. *Teploenergetika* **6,** 46–51.

SYCHEV, V. V. 1961 Sound velocity in water and water vapour on the saturation line. *Ingenerno Physich. Zh.* **4,** 64–69.

VIGLIN, A. I. 1938 Propagation of perturbations in a two-phase liquid–vapour system. *Zh. tekh. Fiz.* **8,** 275–285.

WIJNGAARDEN, L. 1969 On the equations of motion for mixtures of liquid and gas bubbles. *J. Fluid Mech.* **33,** 465–475.